Supplementary information

Influence of crystal shape and orientation on the magnetic microstructure of bullet-shaped magnetosomes synthesized by magnetotactic bacteria

András Kovács[1*], Mihály Pósfai[2,3**], Benjamin Zingsem[1], Zi-An Li[4], Péter Pekker[2], Jan Caron[1], Sandra Prévéral[5], Christopher T. Lefèvre[5], Dennis A. Bazylinski[6], Richard B. Frankel[7]and Rafal E. Dunin-Borkowski[1]

[1] *Ernst Ruska-Centre for Microscopy and Spectroscopy with Electrons, Forschungszentrum Jülich, 52425 Jülich, Germany*
[2] *Research Institute of Biomolecular and Chemical Engineering, University of Pannonia, 8200 Veszprém, Hungary*
[3] *HUN-REN–PE Environmental Mineralogy Research Group, 8200 Veszprém, Hungary*
[4] *State Key Laboratory of Featured Metal Materials and Life-cycle Safety for Composite Structures, and School of Physical Science and Technology, Guangxi University, Nanning 530004, China*
[5] *Aix-Marseille Université, CEA, CNRS, Institute of Biosciences and Biotechnologies of Aix-Marseille, Saint-Paul-lez-Durance, France*
[6] *School of Life Sciences, University of Nevada at Las Vegas, Las Vegas, Nevada, USA*
[7] *Department of Physics, California Polytechnic State University, San Luis Obispo, California, USA*
*, ** Authors for correspondence: a.kovacs@fz-juelich.de, mihaly.posfai@gmail.com

1. Analysis of equilibrium angle of magnetization.

The magnetocrystalline anisotropy energy density F_c is described using the directional cosines l, m, n, where l is the cosine of the angle between the magnetization and the x direction of the chosen coordinate system, m is the cosine of the angle between the magnetization and the y direction, and similarly for n and the z direction. Hence,

$$F_c = K_1(l^2m^2 + m^2n^2 + n^2l^2) + K_2(l^2m^2n^2) \qquad [1]$$

Translated into spherical coordinates, three expressions are obtained for the three different rotations of the crystallographic alignment relative to the elliptical elongation (z axis) of the particles.

<u>100</u>:

If the [100] direction (magnetocrystalline hard axis according to Eq. 1) is parallel to the z axis, then

$$F_c = K_1 \cos^2[\Phi] \sin^4[\Theta] \sin^2[\Phi] + \cos^2[\Theta] \sin^2[\Theta] (K_1 + K_2 \cos^2[\Phi] \sin^2[\Theta] \sin^2[\Phi] \quad [2]$$

where Φ is the azimuthal angle and Θ is the polar angle;

<u>110</u>:

If the [110] direction (magnetocrystalline intermediate/ saddle point according to Eq. 1) is parallel to the z axis, then

$$F_c = {}^{1}/_{256} (2K_2 \sin^2[\Theta] (1 + \sin[2\Phi])(1 + 3\cos[2\Theta] + 2\sin^2[\Theta] \sin[2\Phi])^2 + K_1(53 + 4\cos[2\Theta] + 7\cos[4\Theta] + 24\cos[4\Phi] \sin^4[\Theta] + 16(5 + 7\ \cos[2\Theta]) \sin^2[\Theta] \sin[2\Phi])) \quad [3]$$

<u>111</u>:

If the [111] direction (magnetocrystalline easy axis according to Eq. 1) is parallel to the z axis, then

$$F_c = \left(\left(\frac{K_2}{1728}\right)\left(3\cos[\Theta] + 5\cos[3\Theta] + 4\sin^3[\Theta] (\cos[3\Phi] - \sin[3\Phi])\right)^2\right) + \left(\frac{K_1}{12}\right)\left(4\cos^4[\Theta] + 3\sin^4[\Theta] + 4\cos[\Theta] \sin^3[\Theta] (-\cos[3\Phi] + \sin[3\Phi])\right) \quad [4].$$

In spherical coordinates, the demagnetizing energy density can be described in accordance with Beleggia *et al*. (Beleggia, 2006) as

$$N_{zz} = (\frac{1}{1-r^2})(1 - (r\ arcos[r]/\sqrt{1-r^2}) \quad [5]$$

$$N_{yy} = N_{xx} = \left(\frac{1}{2}\right)(1 - N_{zz}) \quad [6]$$

where r is the aspect ratio of the axes of the ellipsoid (prolate spheroid), assumed to represent the particle shape, such that

$$F_{demag} = \left(\frac{1}{2}\right)\mu_0 M^2 mNm \quad [7]$$

where m is a unit vector along the magnetization direction and N is a tensor composed of the three vectors (N_{xx}, 0, 0), (0, N_{yy}, 0) and (0, 0, N_{zz}).
The total magnetic contribution to the Helmholtz free energy density is

$$F_{total} = F_c + F_{demag} \quad [8]$$

A three-dimensional model for F_{total} 100 at r = 1.1 takes the form:

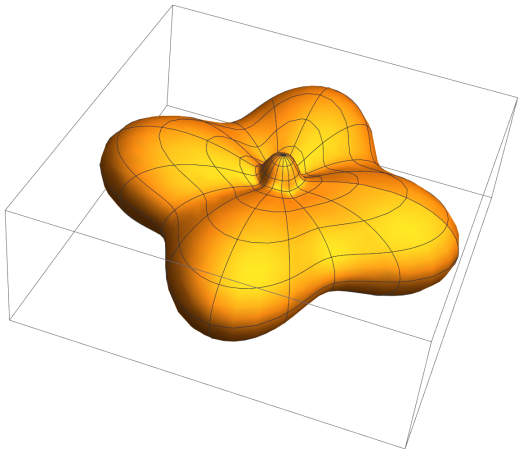

A corresponding three-dimensional model for F_{total} 100 at r = 3 takes the form:

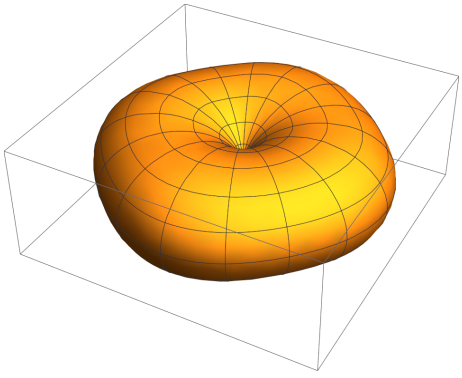

Based on these figures, it is apparent that above a given value of *r* shape anisotropy dominates, creating an easy direction along the *z* axis (*i.e.*, the long axis of the ellipsoid). In the 111 case, the threshold for this condition is trivially less than $r = 1$ (in the oblate regime), since the magnetocrystalline easy axis is already parallel to the shape anisotropy easy axis of the prolate spheroid. For 100 and 110, a threshold greater than $r = 1$ can be identified by calculating the equilibrium angle of magnetization, *i.e.*, the minimum value of F_{total}, as a function of aspect ratio, as shown in Figs 6(e, f).

For the calculations presented here, a saturation magnetization $M_s = 4.8*10^5$ A/m, 1st order cubic anisotropy constant: $K_1 = -1.1*10^4$ J/m^3 and 2nd order cubic anisotropy constant $K_2 = -0.26*10^4$ J/m^3 were used.

2. Electron holography measurement and data processing

Off-axis electron holograms are first recorded from the particles (Fig. S1a) and from a vacuum reference area (not shown) using the same electron beam illumination conditions at magnetic remanence. The Fourier transform of the electron hologram of the sample (not shown) contains a centreband and two sidebands. Reconstruction of the holograms involves digitally selecting one of the sidebands using a virtual aperture followed by centering it in Fourier space and calculating its inverse Fourier transform. The phase of the resulting complex image $\phi = \arctan(i/r)$ is evaluated from the imaginary *i* and real *r* parts of the wavefunction, while the amplitude (Fig. S1b) is obtained from the $A = \sqrt{r^2 + i^2}$. The difference between the object phase and the phase of the vacuum reference hologram is initially evaluated modulo 2π and therefore contains phase discontinuities, which can be "unwrapped" using suitable algorithms. The resulting total phase shift is shown in Fig. S1c. The magnetic contribution (Fig. S1d) to the phase shift is separated from the mean inner potential contribution by taking the difference between two phase maps, between which the magnetization direction in the specimen is reversed *in situ* in the TEM by tilting the sample to ±75° and switching on the ~1.5 T magnetic field of the microscope objective lens, before returning to magnetic-field-free conditions and tilting the sample back to 0° for electron hologram acquisition. The magnetic phase shift map contains the phase variation in radian. Fig. S1e shows an intensity linescan across a particle in the chain. The step in magnetic phase shift is approximately 0.26 radians as shown in Fig. S1e. Finally, using phase differentials, contours and colours are generated, which helps to visualise the magnetic induction map (Fig. S1f).

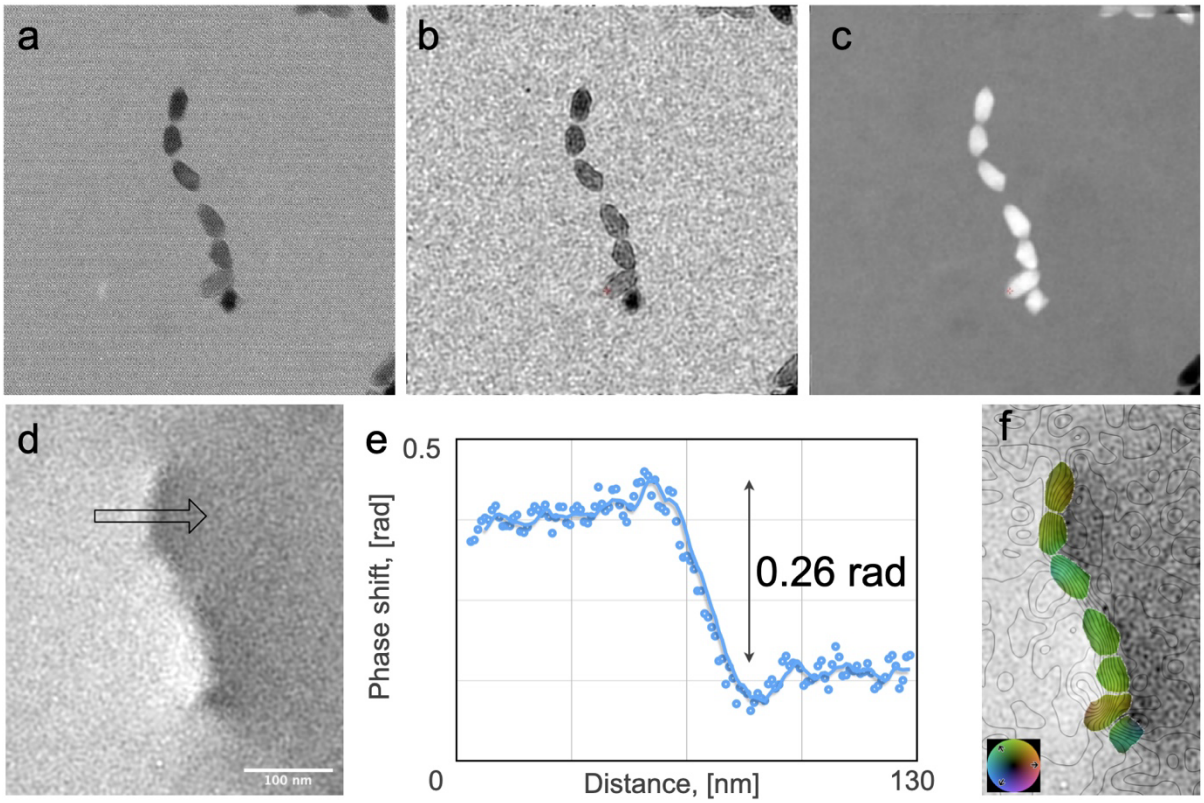

Figure S1. (a) Electron hologram, (b) amplitude image, (c) total phase shift map, (d) magnetic phase shift map, (e) integrated intensity scan across the particle marked by an arrow in (d), (f) magnetic induction. The contour line spacing is 0.0375 radians.